# An FD/FDTD method for optical waveguide modeling

Jon W. Wallace* and Michael A. Jensen
Department of Electrical and Computer Engineering
Brigham Young University
Provo, UT 84602

## I. Introduction

As the complexity of optical devices increases, the need for accurate characterization of mode propagation in these structures is of paramount importance. Complete characterization of electromagnetic wave propagation in arbitrary optical guiding structures generally requires two simulation components: 1) a cross-sectional solver capable of generating modal propagation constants and field profiles for arbitrarily shaped feeding waveguides, and 2) a 3D electromagnetic solver which uses these modes as excitation and simulates the field propagation through the optical device. Prior work has focused on two-dimensional planar waveguide approximations [1], [2] which are inadequate for many geometries or higher-order modes. While the beam propagation method (BPM) [3], [4] has been successfully used for many structures, it is an approximate technique and difficult to implement. Other studies have produced simpler finite-difference (FD) methods for obtaining mode profiles and propagation constants only [5], [6]. In this work, we propose a simple FD method in which Maxwell's time-harmonic equations are discretized directly on a standard Finite-Difference Time-Domain (FDTD) grid to obtain an eigenvalue equation. Direct or iterative solutions can then be used to obtain the modal characteristics. The resulting modal field distributions are subsequently incorporated into FDTD simulations [7], [8] to allow evaluation of reflection and transmission characteristics for arbitrary optical structures.

## II. FD Method

Modal propagation constants and field distributions for a longitudinally homogeneous (in $z$) dielectric waveguide are determined from time-harmonic ($e^{j\omega t}$ temporal variation) forms of Maxwell's equations with $e^{j\beta_z z}$ longitudinal variation, where $\beta_z$ represents the modal propagation constant. For a non-magnetic medium with relative permittivity $\epsilon_r$, two-dimensional Yee [7] discretization of these equations in the $xy$ plane leads to the forms

$$\begin{aligned}
H_{x,ij} &= \tfrac{1}{k_o}\left(j\tfrac{E_{z,ij}-E_{z,i,j-1}}{\Delta y} - \beta_z E_{y,ij}\right) & E_{x,ij} &= \tfrac{1}{\chi^x_{ij}}\left(\beta_z H_{y,ij} - j\tfrac{H_{z,ij+1}-H_{z,ij}}{\Delta y}\right)\\
H_{y,ij} &= \tfrac{1}{k_o}\left(\beta_z E_{x,ij} - j\tfrac{E_{z,ij}-E_{z,i-1,j}}{\Delta x}\right) & E_{y,ij} &= \tfrac{1}{\chi^y_{ij}}\left(j\tfrac{H_{z,i+1,j}-H_{z,ij}}{\Delta x} - \beta_z H_{x,ij}\right) \qquad (1)\\
jH_{z,ij} &= \tfrac{1}{k_o}\left(\tfrac{E_{z,ij}-E_{z,i,j-1}}{\Delta y} - \tfrac{E_{y,ij}-E_{y,i-1,j}}{\Delta x}\right) & jE_{z,ij} &= \tfrac{1}{\chi^z_{ij}}\left(\tfrac{H_{y,i+1,j}-H_{y,ij}}{\Delta x} - \tfrac{H_{x,i,j+1}-H_{x,ij}}{\Delta y}\right)
\end{aligned}$$

where $k_o$ is the free space propagation constant and $\chi^l_{ij} = \epsilon^l_{r,ij}k_o$, with the superscript denoting that the value of the permittivity is evaluated at the location of the $\hat{l}$-polarized electric field component. Additionally, the magnetic field components in Eq. (1) have been normalized by the the free space intrinsic impedance for convenience. If $\beta_z$ is real, the system of equations can be manipulated using purely real arithmetic by making $jE_z$ and $jH_z$ unknowns rather than $E_z$ and $H_z$. In the remainder of the discussion, the FD grid is spatially truncated by assuming the boundary fields decay as $1/\sqrt{R}$, a method which works well for lower order modes.

*II.A Linear Equation Method* A simple strategy for finding modes results from writing (1) as a system of linear equations. Consider a guiding structure possessing a plane of symmetry. If we provide an initial guess for $\beta_z$ and fix one field component at a point in space, we can construct a non-homogeneous linear system of equations. Since the mode structure for this waveguide must possess even or odd symmetry, we can search for the exact mode by perturbing $\beta_z$ and iterating until the field solution from the linear system shows this symmetry. For successful implementation

0-7803-6369-8/00/$10.00 ©2000 IEEE

of this method, the forced field component must be off-center so that symmetry is not artificially introduced. Also, if nearly degenerate modes exist, the forced field components must be chosen with care.

This strategy is particularly well suited for cases where the simulation region contains a large number of cells, since sparse linear equation solvers exist which remain stable for very large systems. In this paper, we used the SuperLU package, which can easily solve for systems of $100 \times 100$ cells on a PC. The main drawbacks of this method are the need for an optimization loop and a good initial guess for $\beta_z$. The next section explains an eigenvalue method which works for any structure, but is less numerically stable.

*II.B Eigenvalue Equation Method* A more direct strategy for finding the modes results from rearranging (1) into an eigenvalue equation. This is accomplished by substituting the equations for $H_z$ and $E_z$ into the remaining 4 equations and subsequently solving for the terms containing $\beta_z$. For example, the equation for $H_{y,ij}$ becomes

$$\begin{aligned}\beta_z E_{x,ij} &= \frac{1}{k_o \Delta x}\left[\frac{H_{y,i+1,j}}{\epsilon^z_{r,ij}\Delta x} - \frac{H_{x,i,j+1}-H_{x,ij}}{\epsilon^z_{r,ij}\Delta y} + \frac{H_{y,i-1,j}}{\epsilon^z_{r,i-1,j}\Delta x} + \frac{H_{x,i-1,j+1}-H_{x,i-1,j}}{\epsilon^z_{r,i-1,j}\Delta y}\right] \\ &\quad + \left[k_o - \frac{1}{k_o \Delta x^2}\left(\frac{1}{\epsilon^z_{r,ij}} + \frac{1}{\epsilon^z_{r,i-1,j}}\right)\right] H_{y,ij}. \qquad (2)\end{aligned}$$

Deriving similar equations for the other 3 field components and combining the unknowns $E_x$, $E_y$, $H_x$, and $H_y$ into the vector $v$ results in a standard eigenvalue equation ($Av = \beta_z v$) that can be solved by a sparse eigenvalue/eigenvector algorithm. Note, however, that for a large number of unknowns this solution may have difficulty converging to the value of $\beta_z$. A good compromise is to use a coarse grid with relatively few unknowns and solve the eigenvalue equation to obtain $\beta_z$. This solution can then be refined using the iterative procedure outlined in Section II.A with a more detailed grid.

*II.C Mode Solution Validation* The validity of this method was assessed by analyzing the lowest order mode in a cylindrical dielectric waveguide with core diameter $d = 5.0\lambda_o$ ($\lambda_o$ is the free space wavelength), core index $n_1 = 1.45$, and cladding index $n_2 = 1.449$. First, the eigenvalue formulation was solved on a $60 \times 60$ cell grid with dimensions $30\lambda_o \times 30\lambda_o$, yielding $\beta_z = 9.104498/\lambda_o$ as compared to the exact value of $\beta_z = 9.104405/\lambda_o$. The absolute error for the field distribution ($x$-component) was small in and near the core (1%) but became large near the domain edges (20%). This solution was refined using iteration with the linear solver on a more detailed grid ($120 \times 120$ cells) having the same dimensions, resulting in $\beta_z = 9.104400/\lambda_o$. Error in the electric field decreased by an order of magnitude (about 2% at the domain edge).

*II.D Mode Solution Example* The proposed solution technique was applied to a rectangular dielectric waveguide with $x$ and $y$ dimensions of $2a = 1\lambda_o$ and $2b = 0.2\lambda_o$ respectively. The refractive index of the core was $n_1 = 3.3$, while that of the cladding was $n_2 = 3.1$. A $40 \times 40$ cell grid was used for the square simulation region ($4\lambda_o$ on a side) in conjunction with the eigenmode solution procedure of Section II.B. The resulting value of $\beta_z$ was then used as a starting point for the method of Section II.A for a grid size of $120 \times 120$ cells. Figure 1 shows the modal field profile for the lowest order mode for this waveguide.

**III. FDTD Simulations**

One advantage of using Yee's discretization scheme for the FD solution is the natural compatibility with FDTD: the resulting modal field distributions can now be directly used to excite the proper mode in the FDTD simulation. In this work, a FDTD implementation in rectangular coordinates is used with a 10 cell perfectly matched layer [8] with quadratically increasing conductivity parameters. The mode is launched by defining a plane normal to the $z$ axis at $z = 0$ which divides scattered

field ($z < 0$) and total field ($z \geq 0$) regions. The relationship between the two regions is given by the previously found mode solution. Accurate computation of $\beta_z$ is essential, since inaccuracies lead to noticeable distortion in the field profile that requires considerable propagation distance (and computation time) to correct. Additionally, this distortion leads to poor characterization of the input field strength which impacts the accuracy of the computed reflection and transmission coefficients. Following completion of the FDTD computation, the reflected and transmitted field profiles are integrated against the eigenmode obtained for the input/output waveguides. Due to the orthonormality of modes, the result of this computation provides the field strengths used to construct the reflection and transmission coefficients.

*III.A Slab Waveguide Misalignment* As a first example of coupling the FD mode solution with the FDTD propagation computation, consider the case of two identical rectangular waveguides with the parameters of the waveguide in Figure 1. The waveguides are end-coupled with various degrees of core misalignment. In cases 1 through 3, the waveguides have a gap (filled with cladding material) between them, are offset in the $x$ dimension, and are offset in the $y$ dimension respectively. Figure 2 shows two-dimensional views of the magnitude of $E_x$ for each of these three computations at fixed values of misalignment. The effect of mode-mismatch and diffraction are evident in these figures. Figure 3 shows the magnitude of the field reflection and transmission coefficients plotted over a range of discontinuity values, where again the mode-mismatch effect is strongly apparent.

*III.B DFB Section* As a final example of the power of the coupled FD/FDTD approach, consider determining the reflection/transmission behavior of a single period of a distributed feedback (DFB) laser cavity. The results of such an analysis could be used in conjunction with one-dimensional solvers to determine the lasing behavior of a very long DFB cavity. Figure 4 provides a side view of the DFB section used in this study, where it is seen that the DFB modulation is performed using a surface relief grating. Adjacent to this illustration is a plot of the $E_x$ field component at one instant of time as the mode propagates through the structure. The resulting reflection and transmission coefficients for the section were $0.0144\angle -84.6°$ and $0.984\angle 180°$, respectively.

## References


[1] D. Marcuse, "Tilt, offset, end-separation loss of lowest-order slab waveguide mode", *Journal of Lightwave Technology*, vol. LT-4, no. 11, pp. 1647-1650, 1986.

[2] S. I. Hosain, J. Meunier, Z. H. Wang, "Coupling efficiency of butt-joined planar waveguides with simultaneous tilt and transverse offset", *Journal of Lightwave Technology*, vol. 14, no. 5, pp. 901-907, 1996.

[3] M. D. Fiet and J. A. Fleck, Jr., "Light propagation in graded-index optical fibers", *Applied Optics*, vol. 17, no. 24, pp 3990-3998, 1978.

[4] W. Huang, C. Xu, S. Chu, S. K. Chaudhuri, "The finite-difference vector beam propagation method: analysis and assessment", *Journal of Lightwave Technology*, vol. 10, no. 3, pp. 295-305, 1992.

[5] P. Lüsse, P. Stuwe, J. Schüle, H. Unger, "Analysis of vectorial mode fields in optical waveguides by a new finite difference method", *Journal of Lightwave Technology*, vol. 12, no. 3, pp. 487-493, 1994.

[6] C. L. Xu, W. P. Huang, M. S. Stern, S. K. Chaudhuri, "Full-vectorial mode calculations by finite-difference method", *IEE Proc.-Optoelectron.*, vol. 141, no. 5, pp. 281-286, 1994.

[7] K. S. Yee, "Numerical solution of initial boundary value problems involving Maxwell's equations in isotropic media", *IEEE Transactions on Antennas and Propagation, AP-14*, pp. 302-307, 1966.

[8] A. Taflove, *Computational Electrodynamics: The Finite Difference Time Domain Method*, 1995.

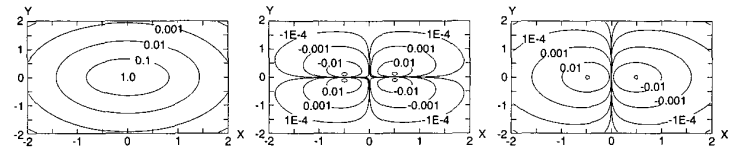

Figure 1: Lowest order $E_x$ mode ($\beta_z = 19.749384/\lambda_0$) in a slab waveguide with width $2a = 1\lambda_o$, height $2b = 0.2\lambda_o$, core index $n_1 = 3.3$, and cladding index $n_2 = 3.1$. Components from left to right are $E_x$, $E_y$, and $E_z$. Dimensions are provided in free space wavelengths.

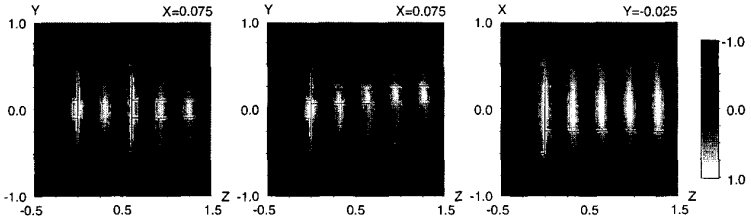

Figure 2: Simulations of mode propagation in the presence of a waveguide discontinuity. Left: Side view of $E_x$ with a gap of $0.6\lambda_o$. Middle: Top view of $E_x$ with an $x$ offset of $0.2\lambda_o$. Right: Side view of $E_x$ with a $y$ offset of $0.16\lambda_o$.

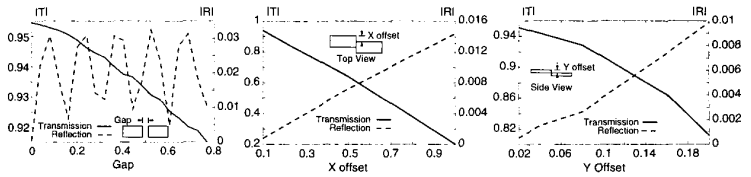

Figure 3: Magnitude of field reflection (R) and transmission (T) coefficients for a range of gap, $x$ offset, and $y$ offset values.

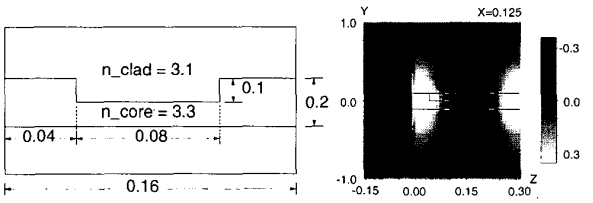

Figure 4: Simulation of a simple DFB grating. The plot on right shows the $E_x$ component.